Interactome analysis of *Caenorhabditis elegans* synapses by TurboID-based proximity labeling

Murat Artan[1], Stephen Barratt[1], Sean M. Flynn[2], Farida Begum[2], Mark Skehel[2], Armel Nicolas[1], and Mario de Bono[1,*]

From the [1]Institute of Science and Technology, Klosterneuburg, Austria and [2]the Cell Biology Division, Medical Research Council Laboratory of Molecular Biology, Cambridge, United Kingdom

Edited by Enrique De La Cruz

Proximity labeling provides a powerful *in vivo* tool to characterize the proteome of subcellular structures and the interactome of specific proteins. The nematode *Caenorhabditis elegans* is one of the most intensely studied organisms in biology, offering many advantages for biochemistry. Using the highly active biotin ligase TurboID, we optimize here a proximity labeling protocol for *C. elegans*. An advantage of TurboID is that biotin's high affinity for streptavidin means biotin-labeled proteins can be affinity-purified under harsh denaturing conditions. By combining extensive sonication with aggressive denaturation using SDS and urea, we achieved near-complete solubilization of worm proteins. We then used this protocol to characterize the proteomes of the worm gut, muscle, skin, and nervous system. Neurons are among the smallest *C. elegans* cells. To probe the method's sensitivity, we expressed TurboID exclusively in the two AFD neurons and showed that the protocol could identify known and previously unknown proteins expressed selectively in AFD. The active zones of synapses are composed of a protein matrix that is difficult to solubilize and purify. To test if our protocol could solubilize active zone proteins, we knocked TurboID into the endogenous *elks-1* gene, which encodes a presynaptic active zone protein. We identified many known ELKS-1-interacting active zone proteins, as well as previously uncharacterized synaptic proteins. Versatile vectors and the inherent advantages of using *C. elegans*, including fast growth and the ability to rapidly make and functionally test knock-ins, make proximity labeling a valuable addition to the armory of this model organism.

Characterizing the interactomes of specific proteins, and the proteome profiles of subcellular structures, cells, and tissues, provides a powerful entry point to probe molecular function. Several methods designed to highlight protein–protein interactions (PPIs) have proven useful, including yeast-two-hybrid (Y2H), affinity purification, and phage display (1–5). However, each method has limitations that can include high false-positive rates, poor detection of transient or weak interactors, a low signal-to-noise ratio when detecting PPIs in specific cell types or subcellular compartments, artifacts created during tissue homogenization, and competing requirements for solubilizing proteins while keeping complexes intact (1, 2). Proximity-labeling methods overcome many of these limitations (1, 6–8) and have allowed the proteomes of subcellular compartments (1) and weak or transient PPIs to be characterized *in vivo* (1). Proximity labeling fuses a protein of interest to an enzyme domain that promiscuously tags proteins in its vicinity with a biochemical handle. This handle allows selective recovery of tagged proteins, which can then be identified by mass spectrometry (MS) (1, 2, 7). The enzyme domains most widely used for proximity labeling in living cells and organisms are engineered variants of the *E. coli* biotin ligase BirA, *e.g.*, BioID and TurboID, or of ascorbate peroxidase, *e.g.*, APEX. *In vivo* applications in animals have, however, been relatively limited (9, 10) and required genetic modifications to alter cuticle permeability in the nematode (11, 12) and tissue dissection to increase H_2O_2 delivery to tissues (13) or pretreatment of live samples with detergent to increase biotin-phenol permeability in the fly (14).

Caenorhabditis elegans has proven a useful workhorse to investigate metazoan biology, offering powerful genetics, *in vivo* cell biology, an anatomy described at electron micrograph resolution, and a defined number of cells whose gene expression can be profiled at single cell resolution (15–18). The ability to probe protein complexes *in vivo* using proximity labeling would add a new dimension to studies in this animal. *C. elegans* offers advantages for proximity labeling. Fusion protein knock-ins can be generated easily and functionally tested. Gram quantities of worms can be grown quickly and cheaply. If desired, proximity labeling can be restricted to specific cell types, using appropriate promoters (18–20). Interacting proteins can be rapidly interrogated using CRISPR/Cas9-generated gene knockouts or knockdowns, *e.g.*, using auxin-induced degradation (21).

---

* For correspondence: Mario de Bono, mdebono@ist.ac.at.
Present address for Murat Artan, Stephen Barratt, Armel Nicolas, and Mario de Bono: Institute of Science and Technology (IST) Austria, Klosterneuburg, Austria.
Present address for Sean M Flynn: Cancer Research UK, Cambridge Institute Li Ka Shing Centre, University of Cambridge, Cambridge, United Kingdom.

C. elegans grows optimally at 15–25 °C. BioID functions poorly at temperatures below 37 °C (22), making it suboptimal for use in the nematode. To date, there is no report applying BioID in *C. elegans*. However, BirA expressed in specific *C. elegans* tissues can biotinylate coexpressed proteins fused to an Avi tag, a 15-residue peptide substrate of BirA (23). The biotinylated Avi-tag fusion protein can then be affinity purified (AP) and coimmunoprecipitating proteins identified by MS (24). Reinke *et al.* (11, 12) expressed cytosolic or nuclear APEX in various *C. elegans* tissues and characterized the corresponding proteomes. APEX has not, however, been used to study PPIs in worms. The APEX peroxidase is promiscuous, labeling proteins far from the APEX-tagged protein and leading to specificity problems (25). Two other studies characterized tissue proteomes in *C. elegans* by expressing mutant phenylalanyl (Phe) tRNA synthetase (MuPheRS) (26, 27). MuPheRS can charge Phe tRNAs with azido-phenylalanine, so that this noncanonical amino acid can be incorporated into proteins during translation. Click chemistry permits the azido group to be derivatized and labeled proteins affinity purified for mass spectrometry. These studies highlighted the proteome of various tissues, including neurons. MuPheRS cannot, however, be used to study PPIs.

Variants of BioID that are more catalytically active, called TurboID and miniTurbo, have recently been developed using directed evolution (28). Expressing either variant in *C. elegans* results in robust biotinylation signals in the intestine, with the strongest signals generated by TurboID (28). However, the authors did not publish interactome or proteomic data for *C. elegans*. A recent study used TurboID to characterize the interactome of the microtubule-binding protein patronin, but ectopically overexpressed this fusion protein in the largest tissue of the animal, the gut, and did not seek to optimize the protocol (29).

Here, we optimize a protocol for TurboID-based proximity-labeling in *C. elegans*. We express TurboID in different *C. elegans* tissues and in the pair of AFD thermosensory neurons. We also knock TurboID into *elks-1*, which encodes a presynaptic active zone protein. We characterize tissue proteomes and highlight tissue-specific proteins. Targeting TurboID to AFD neurons highlights the AFD-specific proteins GCY-8, TTX-1, and GCY-18, and previously uncharacterized proteins that we show are selectively expressed in AFD. The ELKS-1-TurboID samples are enriched in the synaptic proteins UNC-10/RIM, SYD-1/SYDE1, SYD-2/liprin-alpha, SAD-1/BRSK1, CLA-1/CLArinet, C16E9.2/Sentryn, RIM-binding protein RIMB-1, and previously uncharacterized proteins, which we show localize at synapses. Our results indicate that TurboID-mediated proximity labeling can effectively identify the proteome of a pair of neurons and bona fide interactors of a synaptic protein in *C. elegans in vivo*.

Results

Optimizing proximity labeling using TurboID in C. elegans

To examine the extent to which TurboID biotinylates proteins in *C. elegans* (Fig. 1A), we generated transgenic animals expressing a TurboID-mNeongreen-3xFLAG (TbID-mNG) fusion protein in various tissues (Fig. 1B). We compared protein biotinylation levels in age-synchronized young adults expressing the neuronal *rab-3p::TbID-mNG* transgene with wild-type controls. In the absence of exogenously added biotin, transgenic animals showed only a slight increase in biotinylated proteins compared with controls. Adding exogenous biotin increased protein biotinylation specifically in animals expressing the *rab-3p::TbID-mNG* transgene (Fig. 1C). To optimize biotin availability to worm tissues, we treated animals with exogenous biotin for different time intervals, using biotinylation in neurons as a readout. A 2-h incubation was sufficient to achieve robust protein labeling (Fig. 1D). To identify an optimum biotin concentration for protein labeling, we treated animals with varying concentrations of biotin for 2 h. We observed a substantial increase in biotinylation in worms treated with 1 mM biotin but higher biotin concentrations did not appear to further increase biotinylation (Fig. 1E). We also used the *E. coli* biotin auxotrophic strain MG1655 as a food source for worms instead of standard OP50 (30), to minimize the free biotin available prior to addition of exogenous biotin, allowing for tighter control of the time window during which promiscuous biotinylation occurs.

Robust biotinylation in different C. elegans tissues expressing TurboID

Like pan-neuronal expression, intestinal, hypodermal, and muscle-specific expression of TurboID-mNG conferred robust biotinylation activity (Fig. 2A), indicating that TurboID is functional in all major *C. elegans* tissues.

We next optimized a protocol to extract and affinity purify biotinylated proteins from *C. elegans* (Fig. S1, A–C). A significant advantage of PL compared with IP is that extracts can be collected under strong denaturing conditions (1% SDS, 2M urea), since the biotin tag is covalently attached. This allowed us to achieve >95 % solubilization of proteins (Fig. S1, A–C, Experimental procedures). We achieved efficient protein extraction using a cryomill and processed from 5 g to <500 mg of worms. Using 500 mg of worms was typically sufficient to obtain enough material for MS. Age-synchronized young adult worms were incubated with 1 mM of biotin for 2 h at room temperature and immediately frozen after three washes with M9 buffer. Total protein lysate was extracted from powdered worm samples and passed through desalting columns to eliminate free biotin. Removing free biotin was key for successful affinity purification. The flow through was incubated with streptavidin Dynabeads to affinity purify biotinylated proteins (see Experimental procedures). Western blot analysis showed capture of the majority of biotinylated proteins from the whole lysate using our affinity purification protocol (Fig. S2A). After extensive washing and elution, we fractionated the affinity-purified biotinylated proteins by SDS-PAGE, visualized the proteins by Coomassie staining, and analyzed gel slices by LC-MS/MS analysis (Fig. S2B). Using a threshold of at least two unique peptides, we cumulatively identified
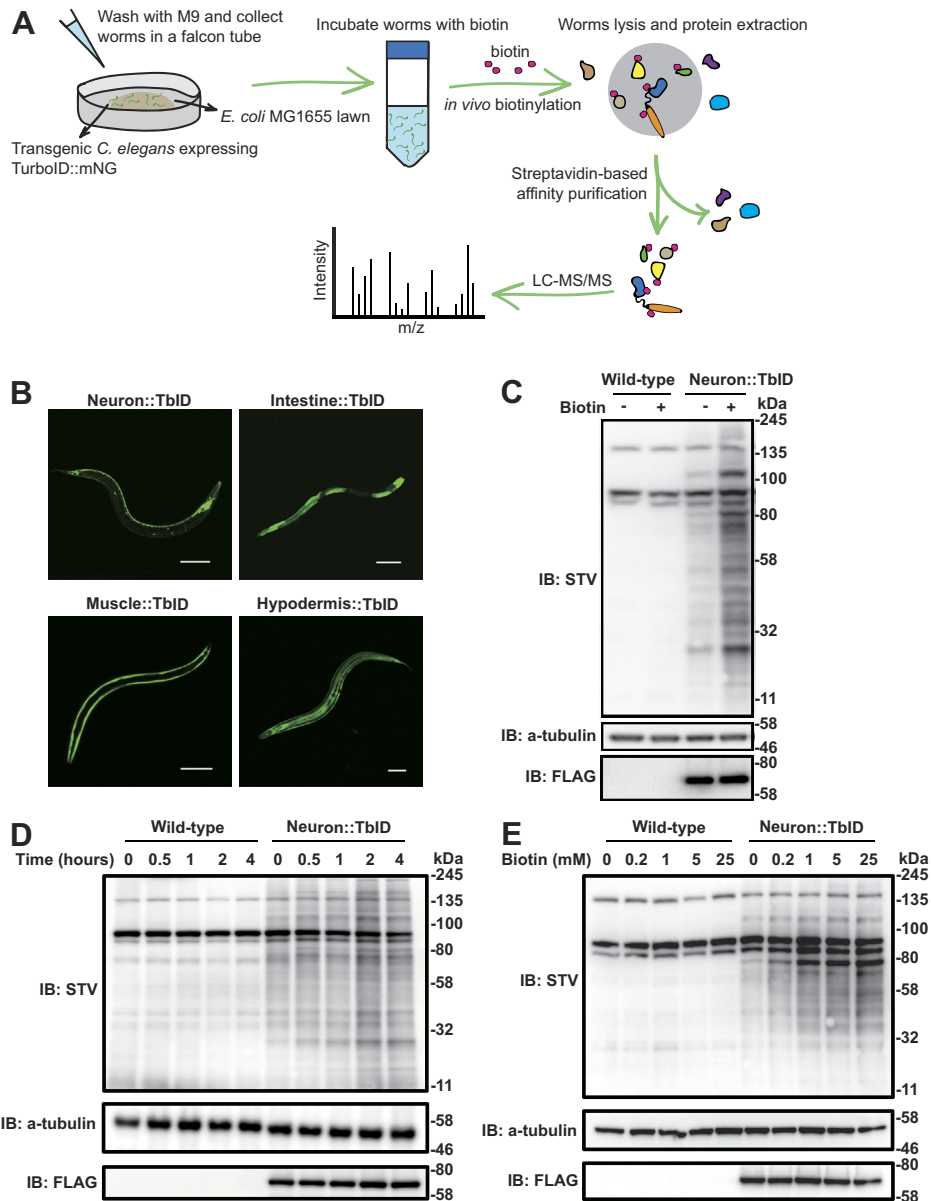
Figure 1. Optimizing TurboID-mediated proximity labeling in *C. elegans*. *A*, schematic overview of TurboID-mediated proximity labeling workflow in *C. elegans*. *B*, transgenic *C. elegans* expressing a free TurboID::mNeongreen::3xFLAG fusion protein selectively in neurons (*rab-3p*), intestine (*ges-1p*), body wall muscle (*myo-3p*), and hypodermis (*dpy-7p*). *C*, western blot analysis of biotinylation by TurboID in the nervous system (*rab-3p::TbID*) in the presence or absence of excess exogenous biotin. Please note that TurboID::mNeongreen fusion protein also contains a FLAG tag. *D* and *E*, analyses of how labeling time (*D*) and exogenous biotin concentration (*E*) alter biotinylation in animals expressing TurboID pan-neuronally. Wild-type worms are shown as controls. Scale bars: 100 μm.

>4000 proteins expressed in one or more tissues (Fig. 2, *B* and *C*, Table S1). Using tissue enrichment analysis (31), we looked for overrepresented annotations in the lists of proteins we identified as unique to each tissue. As expected, terms associated with the targeted tissue were overrepresented in each case, confirming the validity of the method for large tissues (Fig. S3A). In addition, we observed a strong correlation between the two replicates at the level of spectral counts (Fig. S3B). Consistent with previous findings, we identified most proteins in the intestine, followed by the hypodermis and muscle cells (Fig. 2B), (12). Over 2000 proteins were enriched at least 2-fold in one tissue over other tissues (Figs. 2B), and

1274 proteins were detected in only one tissue (Fig. 2C). Proteins identified by MS/MS when TurboID was targeted to neurons included broadly expressed neuronal proteins, such as CLA-1, UNC-31, and proteins expressed in subsets of neurons, such as the glutamate decarboxylase UNC-25, which is known to be expressed in 26 neurons, and OSM-10, which is expressed in four pairs of neurons (Fig. 2D). Muscle-specific samples were enriched in CPNA-1, CPNA-2, PQN-22, and F21C10.7 (Fig. 2D); intestine-specific samples were enriched in ACOX-2, CGR-1, C49A9.9, and C49A9.3 (Fig. 2D), and hypodermis-specific samples included F17A9.5, PAH-1, R05H10.1, and CPN-2 (Fig. 2D). In addition, we identified
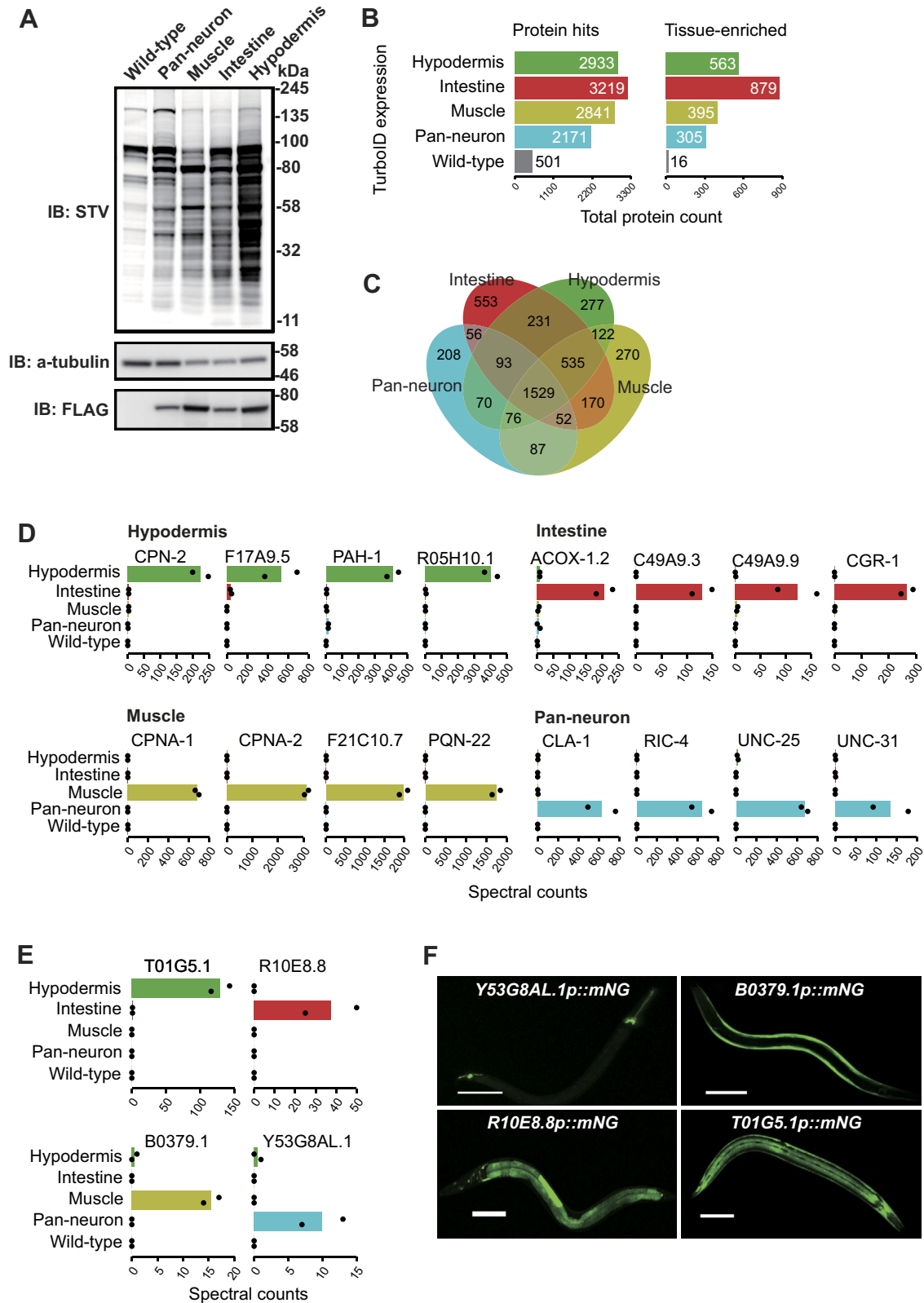
Figure 2. Proteomic analysis of major *C. elegans* tissues. *A*, western blot of lysates obtained from animals expressing free TurboID specifically in the neurons, muscle, intestine, and hypodermis. *B*, total, tissue-enriched, and tissue-specific proteins detected in various tissues by mass spectrometry. Tissue enrichment is defined as proteins with 2-fold or greater mean spectral counts compared with the second-ranked sample. Tissue-specific proteins were uniquely identified in the corresponding tissue. *C*, Venn diagram showing the distribution of protein hits between samples. *D*, mean spectral count of representative proteins in various tissues obtained *via* mass spectrometry. *E* and *F*, mean spectral counts of the proteins Y53G8AL.1, B0379.1, T01G5.1, and R10E8.8 encoded by genes predicted by our TurboID experiments (*E*), and confocal microscopy images of worms expressing mNeongreen from the promoters of these genes (*F*). Scale bars: 100 μm.

tissue-specific enrichment for many proteins whose expression was previously uncharacterized (Table S1, Fig. 2E). For some of these proteins we validated the tissue-selective expression highlighted by our MS/MS data by making transgenic reporters. The reporters confirmed the expression profile predicted by MS/MS, validating the method's specificity (Fig. 2F).

TurboID can identify proteins expressed in only a pair of C. elegans neurons

The *C. elegans* nervous system includes 118 classes of neurons, with most classes consisting of a single pair of neurons that form left/right homologs (16). We asked whether our protocol had sufficient sensitivity to characterize proteins expressed in a single pair of neurons. To test this, we transgenically expressed free TurboID-mNeongreen specifically in the AFD pair of ciliated sensory neurons, using the *gcy-8* promoter (Fig. 3A). Western blot analysis of extracts from

these animals revealed a biotinylation signal significantly higher than that in extracts from wild-type controls (Fig. 3B). Correlation plots of mass spectrometry data obtained for affinity-purified extracts made from animals expressing the *gcy-8p::TbID-mNG* transgene showed reproducible results between replicates (Fig. S4A). As expected, these samples were enriched for proteins specifically or selectively expressed in AFD neurons when compared with similarly processed extracts from nontransgenic controls, or from animals expressing a *rab-3p::TbID-mNG* transgene (Figs. 3C and S4B). Enriched proteins included the transmembrane guanylate cyclases GCY-8 and GCY-18 and the homeobox transcription factor TTX-1 (Figs. 3D and S4B). Our MS data also identified other proteins enriched in the AFD-specific TurboID samples compared with the pan-neuronal TurboID controls (Table S1, Figs. 3E and S4C). To examine if these proteins were selectively expressed in AFD neurons, we generated transgenic reporter lines (Fig. 3F). *nex-4* and F37A4.6 were expressed
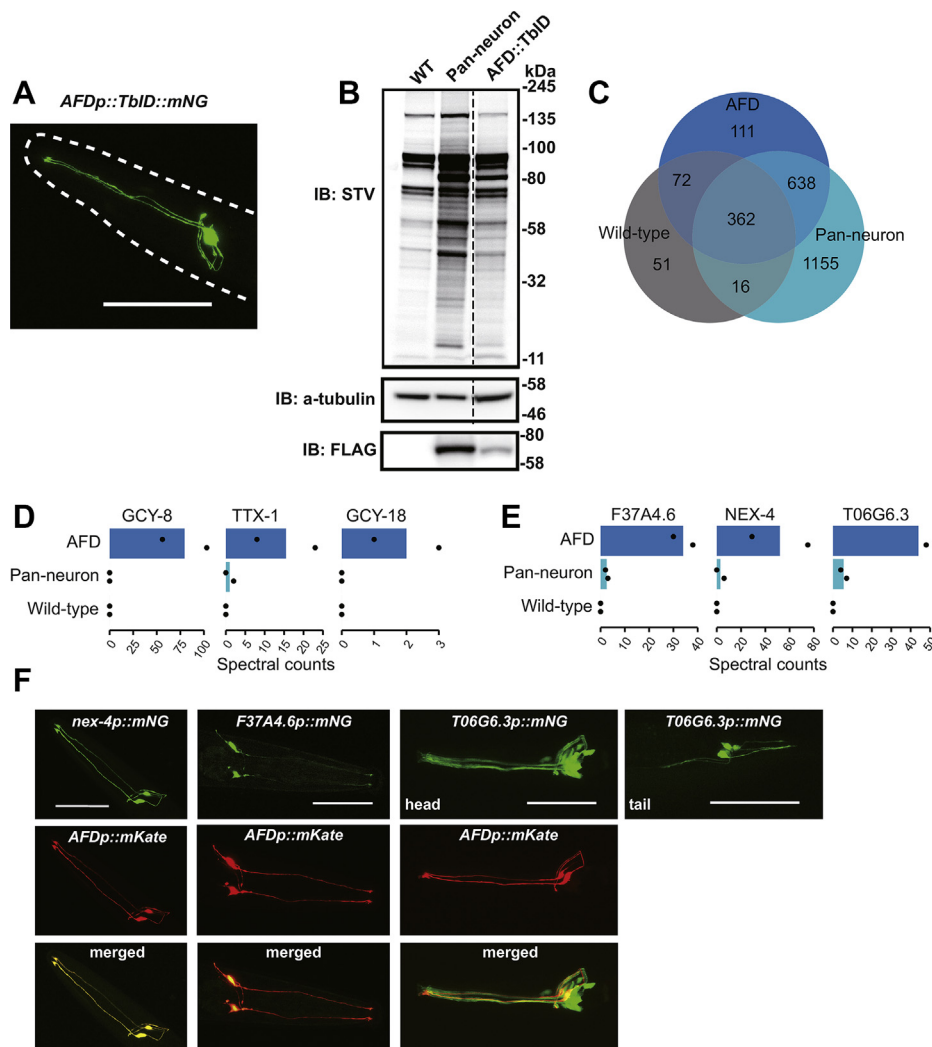

Figure 3. Proteomic analysis of the AFD sensory neuron pair. *A*, confocal microscopy image of *C. elegans* expressing TurboID::mNeongreen fusion protein specifically in the AFD neurons. *B*, western blot analysis of worm lysates obtained from samples expressing free TurboID in AFD neurons, all neurons or none (WT). *C*, Venn diagram showing the distribution of protein hits between samples. *D*, the AFD markers GCY-8, TTX-1, and GCY-18 are highly enriched in AFD::TurboID samples. *E*, NEX-4, F37A4.6, and T06G6.3 proteins were highly enriched in AFD::TurboID samples. *F*, Confocal microscopy images of *C. elegans* expressing *nex-4p::mNeongreen*, *F37A4.6p::mNeongreen* and *T06G6.3p::mNeongreen* transgenes. A *gcy-8p::mKate* transgene was used as a fiducial marker to identify AFD neurons. *A* and *F*, scale bars: 50 μm.

specifically in AFD, albeit F37A4.6 at low levels; T06G6.3 was expressed in a small subset of neurons that included AFD (Fig. 3F). Our list of AFD-enriched proteins, identified by mass spectrometry, was consistent with AFD-specific gene expression identified by RNA Seq (32). These data suggest that TurboID is a reliable tool to map the proteome of specific neurons in *C. elegans*.

Identifying the interactome of a presynaptic protein by TurboID

We next asked if TurboID can highlight the interactome of a specific *C. elegans* protein expressed at endogenous levels. We focused on the synaptic protein ELKS-1, an ortholog of human ERC2 (ELKS/RAB6-interacting/CAST family member 2). ELKS-1 is expressed throughout the nervous system and localizes to the presynaptic active zone, in proximity to other presynaptic proteins such as α-liprin and RIM (33). To have endogenous levels of expression, we knocked *TurboID::m-Neongreen* into the *elks-1* locus using Crispr/Cas9-mediated genome editing. As expected, ELKS-1:: TbID-mNG localized to the nerve ring and other regions rich in synapses (Fig. 4A). Western blot analysis of extracts from ELKS-1::TbID animals did not show an increased biotinylation signal compared with wild-type controls (Fig. 4B). However, mass spectrometry analysis of streptavidin-purified proteins from this knock-in strain revealed enrichment of known synaptic proteins including UNC-10/RIM, SYD-1/SYDE1, SYD-2/α-liprin, SAD-1/BRSK1, CLA-1/CLArinet, C16E9.2/Sentryn, and the RIM-binding protein RIMB-1 (Fig. 4D). We measured enrichment by comparing mass spectrometry data obtained for control extracts processed in parallel from wild-type and from transgenic animals expressing free TurboID-mNG throughout the nervous system, *rab-3p::TbID-mNG* (Fig. 4C and S4E) or both nervous system and other tissues (Fig. S4G). Between-replicate correlation plots revealed reproducible results between experimental repeats (Fig. S4D). We also identified several previously uncharacterized proteins as enriched in ELKS-1::TbID-mNG samples (Table S1, Fig. 4E and S4, F and G). We expressed mNeongreen translational fusion transgenes for several of these proteins exclusively in the AFD neuron pair and showed that they colocalized with ELKS-1::mScarlet at presynaptic active zones where AFD is known to synapse with AIY interneurons (16, 34) (Fig. 4, E and F; highlighted with red dots). Together, our findings show that TurboID-mediated proximity labeling is an effective method to reveal protein interactors in *C. elegans* at endogenous levels with specificity and sensitivity.

Discussion

We optimize the recently developed TurboID-based proximity-dependent protein labeling approach for *C. elegans*, and show that it permits single neuron proteomics and characterization of the interactome of a synaptic protein expressed at endogenous levels. We create reagents that allow TurboID to be applied to different *C. elegans* tissues and identify >4000 proteins expressed in at least one tissue. We were able to

identify proteins expressed exclusively in the AFD neurons and previously uncharacterized proteins that are synaptically localized in the vicinity of ELKS-1.

Proximity labeling methods such as TurboID label interactors throughout the life of the fusion protein. In *C. elegans*, many transgenic experiments use multicopy arrays that typically overexpress the protein of interest. This can lead to inappropriate protein localization, expanding the list of interactors identified by proximity labeling. Expressing bait proteins at physiological levels, and confirming appropriate subcellular localization of the fusion protein, will likely be important to minimize such confounds. Expressing ELKS-1::TurboID at physiological levels, using knock-in strains, identified many proteins predicted to be enriched in the vicinity of ELKS-1. These include known interactors of ELKS-1 in the presynaptic active zone of *C. elegans* neurons. We characterize three proteins, C11E4.6, C03H5.6, and H06I04.1, enriched in proteins biotinylated by ELKS-1::TurboID further and confirm they are synaptically localized. C11E4.6 is predicted to be an 1170 residue protein orthologous to human ANKS1A and ANKS1B (ankyrin repeat and sterile alpha motif domain-containing). Human ANKS1B, also known as AIDA-1, is a risk locus for autism and neurodevelopmental defects (35) and is enriched at postsynaptic densities, where it binds N-methyl-D-aspartate receptors (NMDA) and the adapter protein PSD-95 (36). Our data are consistent with this family of proteins also being enriched presynaptically. Previous studies have reported colocalization of AIDA-1 with the presynaptic excitatory marker VGLUT1 in mossy fiber endings onto CA3 neurons (37), and some presynaptic proteins coimmunoprecipitate with AIDA-1 including the CLA-1 homolog Bassoon (35). C03H5.6 is predicted to encode a 349 residue protein that contains BTB/POZ domains; little is known about this protein's function. H06I04.1 is predicted to encode four isoforms ranging from 231 to 428 residues and contains five coiled-coil domains. Similar to C03H5.6, little is known about this protein's function. Transgenic animals overexpressing C11E4.6 exhibit an uncoordinated phenotype, supporting the idea that it is a synaptic protein. It would be interesting to investigate whether C11E4.6, C03H5.6, or H06I04.1 has a role in synaptic transmission. Another protein that our TurboID data suggest is proximal to ELKS-1 is C16E9.2, the *C. elegans* ortholog of human KIAA0930. C16E9.2 was recently given the name sentryn (STRN-1). STRN-1 together with the SAD kinase and liprin-α promote dense-core vesicle (DCV) pausing at presynaptic regions (38) and optimize localization of synaptic vesicles at the active zone (39).

Some proteins identified in the ELKS-1 proximity labeling experiments are usually considered nonneuronal. We speculate some of these proteins may also be expressed in neurons. For example, we find components of the muscle dense body, including the myotilin ortholog KETN-1/MYOT, the ALP-Enigma protein ALP-1, the sorbin homolog SORB-1, and ZYXin ZYX-1 (40) enriched in both muscle-specific and ELKS-1 samples. Annotations in Wormbase (https://wormbase.org/) also suggest that these proteins are
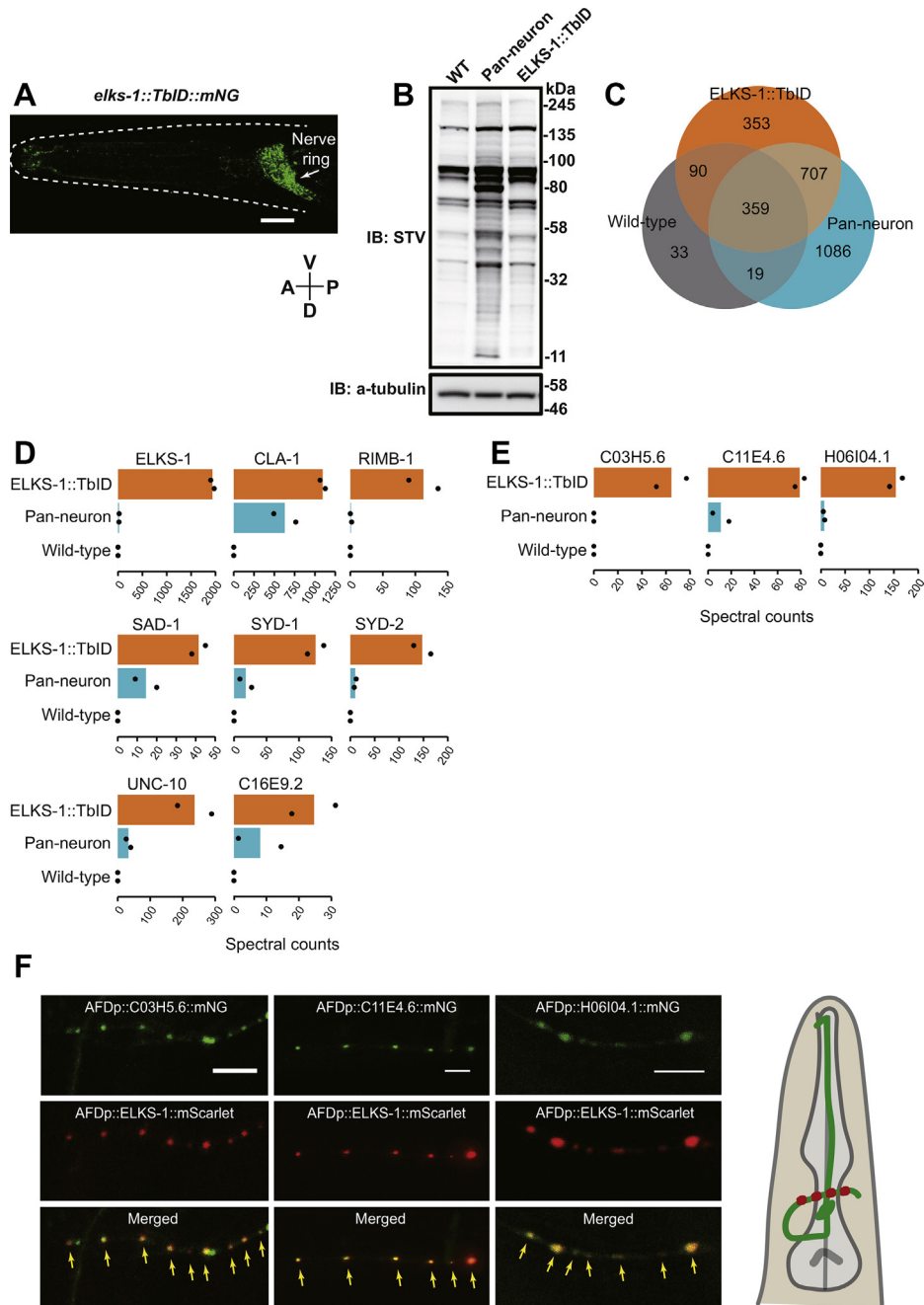
Figure 4. Interactome analysis of the presynaptic active zone protein ELKS-1. *A*, confocal microscopy image of *C. elegans* harboring an *elks-1::TurboID::mNeongreen* knock-in allele generated by CRISPR/Cas9-mediated genome editing. The nerve ring, where many synapses are located, is marked with a *white arrow*. *B*, western blot analysis of lysates obtained from animals expressing the ELKS-1::TurboID::mNeongreen fusion protein. *C*, Venn diagram showing the distribution of protein hits between samples. *D*, the synaptic proteins ELKS-1/ELKS, UNC-10/RIM, SYD-1/SYDE1, SYD-2/liprin-alpha, SAD-1/BRSK1, CLA-1/CLArinet, C16E9.2/Sentryn, and RIM binding protein RIMB-1 were highly enriched in ELKS-1::TurboID samples. *E*, C03H5.6, C11E4.6 and H06I04.1 were highly enriched in ELKS-1::TurboID samples. *F*, confocal microscopy images of transgenic *C. elegans* expressing *C03H5.6::mNeongreen*, *C11E4.6::mNeongreen* and *H06I04.1::mNeongreen* translational fusions in the AFD neuron pair. *elks-1::mScarlet*, used as a control to mark AFD synapses, confirms these proteins are synaptic. Scale bars: 10 μm (*A*) and 5 μm (*F*).

expressed in neurons. Such hypotheses raised by the MS data need to be directly tested, for example, using colocalization studies with fluorescently tagged reporters.

An important variable for TurboID protocols is the delivery of biotin or biotin derivatives. In cultured mammalian cells expressing TurboID or miniTurbo, adding biotin for as little as 10 min yields robust biotinylation (28). In *C. elegans*, adding

biotin to plates seeded with bacteria (*E. coli* OP50 or NA22 strains) is sufficient to promote TurboID labeling, but long incubation times are required to achieve detectable protein biotinylation (28; our data). We find that a 2-h incubation with exogenous biotin is sufficient for strong TurboID signals in worm neurons (Fig. 1*D*). Since in the lab *C. elegans* is typically grown on *E. coli* as a food source, feeding biotin-auxotrophic *E. coli* to

worms provides some control over the start of biotinylation by TurboID. For time-sensitive experiments, it may be possible to soak worms in a buffer containing biotin for shorter periods, *e.g.*, 30 or 60 min and still achieve robust protein biotinylation, although further analysis using MS is required to confirm this.

About 27% of the *C. elegans* proteome comprises integral membrane proteins; however, only 10–11% of the proteins for which we detect peptides correspond to integral membrane proteins. Membrane protein identification is a long-standing problem in mass spectrometry: integral membrane proteins typically yield fewer tryptic peptides, due to a paucity of positively charged residues. In TurboID experiments underrepresentation is compounded, since biotinylation occurs on solvent exposed lysine residues. It will be interesting in future work to explore the recovery of membrane proteins when TurboID is targeted to plasma membrane of *C. elegans* cells.

Four endogenously biotinylated carboxylases dominate the biotinylated proteome in TurboID expressing lines, as seen by both Western blot (Fig. S2A) and MS analysis (data not shown). These carboxylases; PCCA-1/PCCA (propionyl coenzyme A carboxylase alpha subunit), PYC-1/PC (pyruvate carboxylase), MCCC-1/MCCC (methylcronotoyl coenzyme A carboxylase), POD-2/ACACA (acetyl coenzyme A carboxylase) were the most abundantly detected proteins in our MS experiments in every condition tested, including controls. Depending on how broadly and strongly we expressed TurboID in *C. elegans* tissues, these carboxylases account for 8%–85% of peptides identified in MS analysis. We aim to knock-in tags into each of these four genes (*pcca-1*, *pyc-1*, *mccc-1*, and *pod-2*), using CRISPR/Cas9 to allow their depletion by affinity purification, thereby increasing the sensitivity of proximity labeling, particularly when the TurboID-tagged protein is expressed in a small number of cells or at low levels.

Despite extensive washing and use of denaturing conditions, streptavidin purified samples retain substantial nonspecific background. Notably, the mass spectrometer identifies many proteins even when we apply our affinity purification protocol to extracts made from control animals that do not express TurboID. These nonspecific contaminant proteins may be sticky and/or expressed at high enough levels to come through to our pipeline. Alternatively, there may be endogenous biotinylation of many proteins beyond the highly abundant carboxylases PCCA-1, PYC-1, POD-2, and MCCC-1. A future priority is to create a comprehensive list of such contaminants. In summary, our findings show that TurboID works well in a wide array of contexts in the worm. TurboID will be a reliable and useful tool for the *C. elegans* community to map the proteomes of specific cells and subcellular structures and to characterize the interactomes of proteins of interest.

Experimental procedures

Strains

Worms were grown at room temperature (22 °C) on nematode growth medium (NGM) plates seeded with the biotin auxotroph *E. coli* MG1655. *C. elegans* husbandry otherwise followed standard laboratory culture conditions (41).

C. elegans strains used in this study include:

N2, the wild-type Bristol strain

AX7647 *dbIs37[rab-3p::mNeongreen::3XFLAG]*

AX7526 *dbIs24[rab-3p::CeTurboID::mNeongreen::3XFLAG]*

AX7542 *dbIs25[ges-1p::CeTurboID::mNeongreen::3XFLAG]*

AX7578 *dbIs28[myo-3p::CeTurboID::mNeongreen::3XFLAG]*

AX7623 *dbIs33[dpy-7p::CeTurboID::mNeongreen::3XFLAG]*

AX7606 dbIs32[gcy-8p::CeTurboID::mNeongreen::3XFLAG]

AX7917 *dbEx1234[T01G5.1p::mNeongreen::3XFLAG; ccRFP]*

AX7922 *dbEx1241[B0379.1p::mNeongreen::3XFLAG; ccRFP]*

AX7928 dbEx1247[Y53G8AL.1p::mNeongreen::3XFLAG; ccRFP]

AX8059 dbEx1266[R10E8.8p::mNeongreen::3XFLAG]

AX7935 dbEx1251[nex-4p::mNeongreen::3XFLAG; ccRFP]; dbEx1253[gcy-8p:: mKate; ccRFP]

AX7937 dbEx1255[F37A4.6p::mNeongreen::3XFLAG; lin-44p::GFP]; dbEx1253[gcy-8p:: mKate; ccRFP]

AX7939 *dbEx1256[T06G6.3p::mNeongreen::3XFLAG]; dbEx1253[gcy-8p:: mKate; ccRFP]*

AX8110 *dbEx1296[gcy-8p::C03H5.6::mNeongreen::3XFLAG; gcy-8p::elks-1 cDNA::mScarlet; lin-44p::gfp]*

AX8111 *dbEx1297[gcy-8p::C11E4.6::mNeongreen::3XFLAG; gcy-8p::elks-1 cDNA::mScarlet; lin-44p::gfp]*

AX8117 *dbEx1300[gcy-8p::H06I04.1 cDNA isoform 1a::mNeongreen::3XFLAG; gcy-8p::elks-1 cDNA::mScarlet; lin-44p::gfp]*

PHX1710 *elks-1(syb1710)*. The *syb1710* allele is a knock-in that expresses ELKS-1 tagged C-terminally with CeTurboID::mNeongreen::3XFLAG.

Molecular biology

TurboID cloning

TurboID codon-optimized for *C. elegans* (42) was synthesized by IDT (Integrated DNA Technologies Inc, Coralville, IA, USA) and includes an N-terminal Gly-Ser rich linker, a c-Myc tag C-terminally, and two artificial introns (N linker::CeTurboID::c-Myc).

C. elegans codon-optimized mNeongreen::3XFLAG tag was cloned using PCR from DG398 pEntryslot2_mNeongreen::3XFLAG::stop, a Multisite Gateway (ThermoFisher) pEntry vector, which was a gift from Dr Dominique Glauser (University of Fribourg).

DNA encoding N linker::CeTurboID::c-Myc and mNeongreen::3XFLAG were stitched together by fusion PCR using primer sequences that encoded a short Gly-Ser linker. The resulting PCR product (N linker::CeTurboID::c-Myc::mNeongreen::3XFLAG) was cloned into position 2 of a Multisite Gateway pDONR vector (ThermoFisher).

The codon-optimized TurboID plasmid is available at Addgene https://www.addgene.org/.

Transcriptional reporters

Promoters for B0379.1 (∼0.9 kbp), T01G5.1 (∼2.1 kbp), Y53G8AL.1 (∼2.5 kbp), nex-4 (∼1.6 kbp), F37A4.6 (∼2.5 kbp), T06G6.3 (∼2.2 kbp), and R10E8.8 (∼1.6 kbp) were amplified from *C. elegans* genomic DNA by PCR and cloned into position

1 of a Multisite Gateway Donor vector (Thermo Fisher). The resulting pEntryslot1 vectors containing these promoters were each mixed with the dg398 pEntryslot2_mNeongreen::3X-FLAG::stop vector, a pEntryslot3 vector containing the *let-858* or *tbb-2* 3′UTR and pDEST (ThermoFisher) in an LR reaction. The resulting expression vectors were injected into the gonad of day 1 adult N2 worms at a concentration of 25 ng/uL.

Cloning uncharacterized ELKS-1 interactors

ORFs for *C03H5.6* (∼2 kbp) and *C11E4.6* (∼6 kbp) were amplified from *C. elegans* genomic DNA by PCR and cloned into a position 2 Gateway donor vector. cDNA for *H06I04.1* isoform a was synthesized by IDT (Integrated DNA Technologies Inc, Coralville, IA, USA) and cloned into a position 2 Gateway donor vector. The resulting pEntryslot2 vectors were mixed with dg397 pEntryslot3_mNeongreen::3XFLAG::stop::unc-54 3′UTR entry vector and a pDEST vector in an LR reaction. *elks-1* cDNA (∼2.5 kbp) was PCR-amplified from a *C. elegans* cDNA library and cloned into a position 2 Gateway donor vector, mixed with *gcy-8* promoter (position 1) and *mScarlet* (position 3) and a pDEST vector in an LR reaction. Resulting expression vectors were injected into the gonad of day 1 adult N2 worms at a concentration of 25 ng/μL.

Integration of extrachromosomal arrays by UV irradiation

Around 100 L4 stage transgenic animals expressing an extrachromosomal array were picked and transferred to unseeded NGM plates. The plates were placed in a UV cross-linker (Stratalinker 1800) with lids removed and exposed to UV (energy setting 300). The irradiated worms were then transferred to seeded plates (10 worms/plate). In total, 200 of their F1 progeny expressing the transgene were picked and individually transferred to a seeded plate. Plates containing many transgenic F2 progeny, indicating potential integration of the transgene, were selected, and eight F2 animals from the candidate plates singled and examined for 100% transmission in the next generation. Integrants were outcrossed to N2 worms at least four times.

Primers used for cloning

myo-3 promoter (∼2.6 kb)

F-myo-3p-Entry1-
GGGGACAACTTTGTATAGAAAAGTTGTGTAGGC
AATCAGTCAAACCGAATAAAA
R-myo-3p-Entry1-
GGGGACTGCTTTTTTGTACAAACTTGTTCTAGA
TGGATCTAGTGGTCGTGGGTT

dpy-7 promoter (∼380 bp)

F-dpy-7p-Entry1-GGGGACAACTTTGTATAGAAAG
TTGAATCTCATTCCACGATTTCTCGCAACACAT
R-dpy-7p-Entry1-GGGGACTGCTTTTTTGTACAAACT
TGTTATCTGGAACAAAATGTAAGAATATTCTTA

gcy-8 promoter (∼940 bp)

F-gcy-8p-Entry1-GGGGACAACTTTGTATAGAAAAGT

TGGGTTCAACAAGGGTATTGTATTGCAATCAGTG
R-gcy-8p-Entry1-GGGGACTGCTTTTTTGTACAAACT
TGTTTGATGTGGAAAAGGTAGAATCGAAAATCC

T01G5.1 promoter (∼2.1 kbp)

F-T01G5.1p-Entry1-   GGGGACAACTTTGTATAGAA
AAGTTGCACCTGAACACAACATTTTCTG
R-T01G5.1p-Entry1- GGGGACTGCTTTTTTGTACAAA
CTTGGACATGAAATTGTATCTGAAAGC

Y53G8AL.1 promoter (∼2.5 kbp)

F-Y53G8AL.1p-Entry1-   GGGGACAACTTTGTATAGA
AAAGTTGGTAGTTATGGAAAAGCAACGTCGGAG
R-Y53G8AL.1p-Entry1-   GGGGACTGCTTTTTTGTACA

AACTTGTCTAAAATAGCATTGGTTCTGAAACTTTG

B0379.1 promoter (∼0.9 kbp)

F-B0379.1p-Entry1- GGGGACAACTTTGTATAGAAAA
GTTGGAAACAATATTATTTTTGTTTCACAG
R-B0379.1p-Entry1- GGGGACTGCTTTTTTGTACAAAC
TTGGTTGTTGTTGTCTCGATGGAAAAG

nex-4 promoter (∼1.6 kbp)

F-nex-4p-Entry1-   GGGGACAACTTTGTATAGAAAAG
TTGCCTGAGAATTACTGAAGTTTAAGC
R-nex-4p-Entry1- GGGGACTGCTTTTTTGTACAAACT
TGCTCGAGTTACTTCAATGCTCACG

F37A4.6 promoter (∼2.5 kbp)

F-F37A4.6p-Entry1-   GGGGACAACTTTGTATAGAAA
AGTTGGATTCAGAAAATTCAGAAAGGCATTC
R-F37A4.6p-Entry1-   GGGGACTGCTTTTTTGTACAA
ACTTGCATTATAGGAAGACTGAGATTCCAAGC

T06G6.3 promoter (∼2.2 kbp)

F-T06G6.3p-Entry1- GGGGACAACTTTGTATAGAAAA
GTTGCATTTTTTGCTCTAAAGGTGGAATAG
R-T06G6.3p-Entry1- GGGGACTGCTTTTTTGTACAAA
CTTGCTTTGAAAAAAGTTCAGAGTAGTAGAG

C03H5.6 genomic DNA (∼2 kbp)

F-C03H5.6-Entry2-   GGGGACAAGTTTGTACAAAAAA
GCAGGCTtttcagaaaaATGTTAGAATGTATACATCC
AACAT
R-C03H5.6-Entry2- GGGGACCACTTTGTACAAGAAAG
CTGGGTATGTACGATTCATCAAACCACCTAC

C11E4.6 genomic DNA (∼6 kbp)

F-C11E4.6-Entry2- GGGGACAAGTTTGTACAAAAAAG
CAGGCTtttcagaaaaATGAGCCTCAAAGACTT
TGTCATATC

R-C11E4.6-Entry2- GGGGACCACTTTGTACAAGAAAG
CTGGGTAATTTCTTTGGTTCTCAGTAGTTTGCTG

H06I04.1 cDNA isoform 1a (∼1.5 kbp)

F-H06I04.1-Entry2- GGGGACAAGTTTGTACAAAAAA
GCAGGCTtttcagaaaaATGAGCAAAGAAACTGGAAA
AATGGCGG

R- H06I04.1-Entry2- GGGGACCACTTTGTACAAGAA
AGCTGGGTAAAATGGTCCAGATCTTGCTTCATT
GGTC

R10E8.8 promoter (∼1.6 kbp)

F-R10E8.8p-Entry1- GGGGACAACTTTGTATAGAAAA
GTTGCACATAAAATACGTTTTAGTAGCTGTCAG
CAC

R-R10E8.8p-Entry1- GGGGACTGCTTTTTTGTACAAA
CTTGTTTTTGTCTGAAAATCGAACATTAAAAATA
ACAGG

elks-1 cDNA (∼2.5 kb)

F-elks-1-cDNA-Entry2-GGGGACAAGTTTGTACAAAA
AAGCAGGCTTTTCAGAAAAATGGCACCTGGTCC
CGCACCATACAGC

R-elks-1-cDNA-Entry2- GGGGACCACTTTGTACAAGA
AAGCTGGGTAGGCCCAAATTCCGTCAGCATCGT
CGTG

rab-3 promoter (∼1.2 kb) and *ges-1* promoter (∼3.4 kb) were used from de Bono lab plasmid collection.

Sequence of TurboID construct

GGAGGTGGTGGATCAGGCTCGGGAGGTCGAGGCT
CAGGATCCGGTTCCGGCTCCGGCTCTGGTTCCGGTT
CGGGTTCCGGTTCTGGAAAGGATAACACCGTTCCAC
TTAAGCTTATCGCCCTTCTTGCCAACGGAGAATTCC
ACTCTGGAGAGCAACTTGGAGAGACTCTTGGAATGT
CCCGTGCTGCCATCAACAAGCATATCCAAACCCTTCG
TGATTGGGGAGTTGATGTTTTCACTGTTCCAGGAAA
GgtaagtttaaacatatatatactaactaaccctgattatttaaattttcagGGATAC
TCCCTTCCAGAGCCAATCCCACTTCTTAACGCCAAGC
AAATCCTTGGACAACTTGATGGAGGATCCGTCGCTG
TCCTTCCAGTTGTTGATTCCACCAACCAATACCTTCT
TGACCGTATCGGAGAGCTTAAGTCTGGAGACGCCTG
CATCGCTGAGTACCAACAAGCTGGACGCGGATCTCG
CGGACGCAAGTGGTTCTCCCCATTCGGAGCCAACCTT
TACCTTTCTATGTTCTGGCGTCTTAAGCGTGGACCAG
CTGCTATCGGACTTGGACCAGTTATCGGAATCGTTAT
GGCTGAGGCCCTTCGTAAGCTTGGATATAAGgtaagtttaa
acagttcggtactaactaaccatacatatttaaattttcagGTTCGTGTTAAGT
GGCCAAACGATCTTTACCTTCAAGACCGTAAGCTTGC
TGGAATCCTTGTCGAGCTTGCTGGAATCACCGGAGA
CGCCGCTCAAATCGTTATCGGAGCTGGAATCAACGTT
GCCATGCGTCGTGTTGAGGAGTCTGTTGTTAACCAA
GGATGGATCACTCTTCAAGAGGCTGGAATCAACCTT
GATCGTAACACCCTTGCTGCCACCCTTATCCGTGAGC
TTCGTGCTGCCCTTGAGCTTTTCGAGCAAGAGGGAC
TTGCCCCATACCTTCCACGCTGGGAGAAGCTTGACA
ACTTCATCAACCGCCCAGTTAAGCTTATCATCGGAGA
TAAGGAATCTTCGGAATCTCTCGCGGAATCGACAAG
CAAGGAGCTCTTCTTCTTGAGCAAGATGGAGTCATT
AAGCCATGGATGGGAGGAGAGATTTCCCTTCGTTCC
GCTGAGAAGGCCGGAGGAGAACAGAAGCTTATAAGT
GAGGAGGACCTGGGATCCGCTGGATCCGCTGCTGGA
TCCGGTGAGTTCATGGTGTCGAAGGGAGAAGAGGAT
AACATGGCTTCACTCCCAGCTACACACGAACTCCAC
ATCTTCGGATCGATCAACGGAGTGGATTTCGATATG
GTCGGACAAGgtaagtttaaacatatatatactaactaaccctgattatttaaat
tttcagGAACTGGAAACCCAAACGATGGATACGAGGAAC
TCAACCTCAAGTCGACAAAGGGAGATGCAATTCTCG
CCATGGATTCTCGTGCCACACATCGGATACGGATTC
CACCAATACCTCCCATACCCAGgtaagtttaaactgagttctacta
actaacgagtaatatttaaattttcagATGGAATGTCACCATTCCAAG
CTGCCATGGTGGATGGATCGGGATACCAAGTTCACC
GAACAATGCAATTCGAGGATGGAGCCTCGCTCAGTG
AACTACCGATACACATACGAGGGATCGCACATCAAG
gtaagtttaaacagttcggtactaactaaccatacatatttaaattttcagGGAGAG
GCTCAAGTTAAGGGAACAGGATTCCCAGCTGATGGA
CCAGTGATGACAAACTCACTCACAGCTGCTGATTGGT
GCCGATCGAAAAAGACATACCCAAATGATAAGACAA
TATCTCGACATTCAAGTGGTCGTACACTACTGGAAAC
GGAAAGCGATACCGATCGACAGCCCGAACAACATAC
ACATTCGCTAAGCCAATGGCCGCCAACTACCTCAAG
gtaagtttaaacatgattttactaactaactaatctgatttaaattttcagAATCAAC
CAATGTACGTGTTCCGAAAGACAGAACTCAAGCACT
CAAAGACAGAGCTGAACTTCAAAGAGTGGCAAAAGG
CCTTCACAGATGTGATGGGAATGGATGAACTCTACA
AGGACTACAAAGACCATGACGGTGATTATAAAGATC
ATGACATCGATTACAAGGATGACGATGACAAG

N/C terminus Gly-Ser rich linkers
CeTurboID
Introns
C-myc
mNeongreen
3XFLAG

Light microscopy

Confocal microscopy images of transgenic *C. elegans* expressing fluorescent proteins were acquired using a Leica (Wetzlar, Germany) SP8 inverted laser scanning confocal microscope with 10× 0.3 NA dry, 63× 1.2 NA water or 63× 1.2 NA oil-immersion objectives, using the LAS X software platform (Leica). The Z-project function in Image J (Rasband, W. S., ImageJ, US National Institutes of Health, http://rsbweb.nih.gov/ij/) was used to obtain the figures used in the panels. Animals were mounted on 2% agarose pads and immobilized with 100 μM of sodium azide.

Immunoblotting

Synchronized populations of *C. elegans* grown on *E. coli* MG1655 were harvested at L4 or young adult stage, washed three times in M9 buffer, incubated at room temperature (22 °C) in M9 buffer supplemented with 1 mM biotin, and *E. coli* MG1655 for 2 h. Two hours later, the worms were washed three times in M9 buffer and flash frozen after the M9 buffer was completely aspirated and 4× Bolt LDS sample buffer supplemented with fresh DTT. The samples were then thawed, boiled for 10 min at 90 °C, vortexed for 10 min, centrifuged for 30 min at 15,000 rpm at 4 °C, and the supernatant collected. Proteins were transferred to a PVDF membrane (Thermofisher Scientific) following electrophoresis using Bolt 4–12% Bis-Tris Plus gels (Thermofisher Scientific). Membranes were blocked for 1 h at room temperature with TBS-T buffer containing 5% BSA and incubated for 2 h at room temperature with HRP-conjugated or fluorescently labeled streptavidin or with HRP-conjugated antibodies. Membranes were then washed three times with TBS-T. The following antibodies or protein-HRP conjugates were used for this study: IRDye 800CW Streptavidin (1:7000 in TBS-T) (LI-COR Biosciences), Anti-FLAG M2-Peroxidase (1:5000 in TBS-T) (A8592 Sigma), anti-alpha tubulin-HRP (1:10,000 in TBS-T) (DM1A Abcam ab40742), Streptavidin-HRP (1:5000 in TBS-T) (3999S Cell Signaling). Membranes were imaged using ChemiDoc the Imaging System (Models MP or XRS+, Bio-Rad).

TurboID-based enzymatic protein labeling and extraction of biotinylated proteins from C. elegans

Gravid adult *C. elegans* were bleached and the eggs transferred to NGM plates seeded with *E. coli* MG1655 to obtain synchronized populations of worms. The animals were harvested at L4 or young adult stage, washed three times in M9 buffer, incubated at room temperature (22 °C) in M9 buffer supplemented with 1 mM biotin, and *E. coli* MG1655 for 2 h unless stated otherwise. Two hours later, the worms were washed three times in M9 buffer and allowed to settle on ice after the last wash. After completely aspirating the M9 buffer, two volumes of RIPA buffer supplemented with 1 mM PMSF and cOmplete EDTA-free protease inhibitor cocktail (Roche Applied Science) were added to one volume of packed worms. The animals were again allowed to settle on ice and then added dropwise to liquid N_2 to obtain frozen worm "popcorn." A Spex 6875D cryogenic mill was used to grind frozen *C. elegans* to a fine powder, which was then stored at −80 °C. Worm powder was thawed by distributing it evenly along the length of a 50 ml falcon tube and rolling it on a tube roller at 4 °C. After the sample was completely thawed, it was centrifuged (1000 rpm, 1 min, 4 °C) to collect the sample at the bottom of the tube. SDS and DTT were added to the sample to final concentrations of 1% and 10 mM respectively, from stock solutions of 20% SDS and 1M DTT. The tubes were gently inverted a few times and immediately incubated at 90 °C for 5 min. After heat treatment, the samples were sonicated continuously for 1 min twice, with brief cooling between the two sonication steps. Sonication used a probe sonicator microtip (MSE Soniprep 150 plus) and an amplitude setting of 16/max. The samples were cooled to room temperature following sonication and adjusted to 2 M urea using a stock solution (8 M urea, 1% SDS, 50 mM Tris-HCl, 150 mM NaCl). The samples were then centrifuged at 100,000g for 45 min at 22 °C, and the clear supernatant between the pellet and surface lipid layer transferred to a new tube.

Zeba spin desalting columns (7K MWCO) (Thermofisher) were equilibrated three times with 5 ml RIPA buffer containing 1% SDS and 2 M urea, freshly supplemented with protease inhibitors (Roche cOmplete EDTA-free protease inhibitor cocktail 1 tablet/25 ml; PMSF 1 mM) by centrifugation at 1000g for 5 min (or until the buffer was completely eluted from resin). Around 4 ml of clarified sample was then loaded onto the equilibrated spin column and desalted by centrifugation at 1000g for 5 min (or until the sample was completely eluted from resin) to remove free biotin. The desalting step was repeated once more using freshly equilibrated columns. Protein concentration in the samples was measured using Pierce 660 nm protein assay reagent supplemented with Ionic Detergent Compatibility Reagent (IDCR) (Thermo Fisher Scientific).

Biotinylated protein pull-down and elution

Dynabeads MyOne streptavidin C1 (Invitrogen, 2 ml bead slurry per 90 mg of *C. elegans* total protein lysate) were equilibrated in RIPA buffer by briefly incubating them three times in the buffer and using magnetic separation to retain beads while discarding buffer (note: we were able to reduce the amount of protein lysate to 5–10 mg in subsequent experiments without compromising the mass spectrometry data). Desalted, clarified samples were combined with Dynabeads in a 50 ml falcon tube and incubated overnight in a tube roller at room temperature. Beads were magnetically separated using a neodymium magnet taped to the tube and incubated on a rocking platform. Unbound lysate was removed and the Dynabeads transferred to 2 ml LoBind protein tubes (Eppendorf). Beads were washed five times with 2% SDS wash buffer (150 mM NaCl, 1 mM EDTA, 2% SDS, 50 mM Tris-HCl, pH 7.4) and five times with 1M KCl wash buffer; beads were transferred to new tubes after each wash.

Elution sample buffer was prepared by dissolving free biotin (Sigma) to saturation in sample buffer (NuPAGE LDS sample buffer 4×) containing reducing agent (NuPAGE sample reducing agent 10×). Elution sample buffer was centrifuged at 13,000 rpm for 5 min to remove undissolved biotin and the elution sample buffer saturated with dissolved biotin was transferred to a new tube. Hundred microliter of elution buffer was applied to Dynabeads, vortexed gently, heated for 5 min at 90 °C, before the vortexing and heating steps were repeated. Dynabeads were separated magnetically and elution buffer containing biotinylated proteins was transferred to a new 1.5 ml LoBind protein tube (Eppendorf). Seventy microliter of sample was electrophoresed on a NuPAGE 4–12% Bis-Tris protein gel (Invitrogen), which was then stained with InstantBlue (Expedeon) for visualization. The gel was sliced into 20 fractions and sent for mass spectrometry analysis.

Mass spectrometry

Polyacrylamide gel slices (1–2 mm) containing the purified proteins were prepared for mass spectrometric analysis using the

Janus liquid handling system (PerkinElmer, UK). Briefly, the excised protein gel pieces were placed in a well of a 96-well microtitre plate, destained with 50% v/v acetonitrile and 50 mM ammonium bicarbonate, reduced with 10 mM DTT, and alkylated with 55 mM iodoacetamide. After alkylation, proteins were digested with 6 ng/μl Trypsin (Promega, UK) overnight at 37 °C. The resulting peptides were extracted in 2% v/v formic acid, 2% v/v acetonitrile. The digest was analyzed by nano-scale capillary LC-MS/MS using an Ultimate U3000 HPLC (ThermoScientific Dionex) to deliver a flow of approximately 300 nl/min. A C18 Acclaim PepMap100 5 μm, 100 μm × 20 mm nanoViper (ThermoScientific Dionex), trapped the peptides prior to separation on an EASY-Spray PepMap RSLC 2 μm, 100 Å, 75 μm × 250 mm nanoViper column (ThermoScientific Dionex). Peptides were eluted using a 60-min gradient of acetonitrile (2% to 80%). The analytical column outlet was directly interfaced *via* a nano-flow electrospray ionization source with a hybrid quadrupole orbitrap mass spectrometer (Q-Exactive Orbitrap, ThermoScientific). Data collection was performed in data-dependent acquisition (DDA) mode with an r = 70,000 (@ m/z 200) full MS scan from m/z 380–1600 with a target AGC value of 1e6 ions followed by 15 MS/MS scans at r = 17,500 (@ m/z 200) at a target AGC value of 1e5 ions. MS/MS scans were collected using a threshold energy of 27 for higher energy collisional dissociation (HCD) and a 30 s dynamic exclusion was employed to increase depth of coverage. Acquired raw files were then searched in MaxQuant (43) (version 1.6.10.43) against a FASTA database containing the *C. elegans* reference proteome from UniProt KB (including SwissProt and TrEMBL entries) downloaded on September 27, 2019. In total, 28,474 accessions were actually searched. We used trypsin, which cleaves peptides at the C-terminal side of lysine and arginine residues, to generate peptide fragments for mass spectrometry. Most parameters were kept at their default value. Carbamidomethyl (C) (+57.0214637236) was set as fixed modification. Variable modifications included were "Oxidation (M)" (+15.9949146221), "Acetyl (Protein N-term)" (+42.0105646863), "Deamidation (NQ)" (+0.9840155848), "Gln->pyro-Glu" (-17.0265491015), "Phospho (STY)" (+79.9663304084), as well as two custom modifications ("K-Biot" and "N-term-Biot", +226.077598394 on, respectively, lysines or protein N-terminus) to account for TurboID-induced biotinylated peptides. Match Between Runs (MBR, not used in the final results) and Second Peptide Search were activated. All FDRs were set to 1%. Identified data was then reprocessed in R using the evidence.txt results table, but a decision was made to exclude indirect, MBR-based identifications to focus on higher confidence hits. The decoy used to establish the FDR was the reverted search database. MaxQuant applies a PSM-level FDR globally as well as per class of modified peptides ("Site decoy fraction), and also at protein level. All three FDR levels were set to 1%.

Ethics Statement

The work used the free-living nematode *C. elegans*, for which there is no requirement for review and approval from an institutional animal care and use committee. Transgenic experiments were carried out following IST guidelines for such work.

Data availability

The mass spectrometry proteomics data have been deposited to the ProteomeXchange Consortium *via* the PRIDE partner repository at http://www.ebi.ac.uk/pride with the dataset identifier PXD027068. Submission details: Project Name: Interactome analysis of *C. elegans* synapses by TurboID-based proximity labeling. Project accession: PXD027068. We have uploaded the mass-labeled MS/MS data on MS Viewer, available at https://msviewer.ucsf.edu/prospector/cgi-bin/msform.cgi?form=msviewer. The key to access the repository is bbfl7oetve. Only ~100,000 of the ~2.5 million spectra obtained in the course of our work are in the database, since replicates are omitted, and the best spectrum retained for each peptide. All remaining data are contained within the article.

References

1. Qin, W., Cho, K. F., Cavanagh, P. E., and Ting, A. Y. (2021) Deciphering molecular interactions by proximity labeling. *Nat. Methods* **18**, 133–143
2. Kim, D. I., and Roux, K. J. (2016) Filling the void: Proximity-based labeling of proteins in living cells. *Trends Cell Biol.* **26**, 804–817
3. Varnaitè, R., and MacNeill, S. A. (2016) Meet the neighbors: Mapping local protein interactomes by proximity-dependent labeling with BioID. *Proteomics* **16**, 2503–2518

4. Trinkle-Mulcahy, L. (2019) Recent advances in proximity-based labeling methods for interactome mapping. *F1000Research.* **8**

5. Rees, J. S., Li, X. W., Perrett, S., Lilley, K. S., and Jackson, A. P. (2015) Protein neighbors and proximity proteomics. *Mol. Cell. Proteomics* **14**, 2848–2856

6. Xu, Y., Fan, X., and Hu, Y. (2021) *In vivo* interactome profiling by enzyme-catalyzed proximity labeling. *Cell Biosci.* **11**, 1–9

7. Samavarchi-Tehrani, P., Samson, R., and Gingras, A. C. (2020) Proximity dependent biotinylation: Key enzymes and adaptation to proteomics approaches. *Mol. Cell. Proteomics* **19**, 757–773

8. Gingras, A. C., Abe, K. T., and Raught, B. (2019) Getting to know the neighborhood: Using proximity-dependent biotinylation to characterize protein complexes and map organelles. *Curr. Opin. Chem. Biol.* **48**, 44–54

9. Uezu, A., Kanak, D. J., Bradshaw, T. W. A., Soderblom, E. J., Catavero, C. M., Burette, A. C., Weinberg, R. J., and Soderling, S. H. (2016) Identification of an elaborate complex mediating postsynaptic inhibition. *Science* **353**, 1123–1129

10. Dingar, D., Kalkat, M., Chan, P. K., Srikumar, T., Bailey, S. D., Tu, W. B., Coyaud, E., Ponzielli, R., Kolyar, M., Jurisica, I., Huang, A., Lupien, M., Penn, L. Z., and Raught, B. (2015) BioID identifies novel c-MYC interacting partners in cultured cells and xenograft tumors. *J. Proteomics* **118**, 95–111

11. Reinke, A. W., Balla, K. M., Bennett, E. J., and Troemel, E. R. (2017) Identification of microsporidia host-exposed proteins reveals a repertoire of rapidly evolving proteins. *Nat. Commun.* **8**, 1–11

12. Reinke, A. W., Mak, R., Troemel, E. R., and Ben, E. J. (2017) *In vivo* mapping of tissue- and subcellular-specific proteomes in Caenorhabditis elegans. *Sci. Adv.* **3**, 1–12

13. Chen, C. L., Hu, Y., Udeshi, N. D., Lau, T. Y., Wirtz-Peitz, F., He, L., Ting, A. Y., Carr, S. A., and Perrimon, N. (2015) Proteomic mapping in live Drosophila tissues using an engineered ascorbate peroxidase. *Proc. Natl. Acad. Sci. U. S. A.* **112**, 12093–12098

14. Mannix, K. M., Starble, R. M., Kaufman, R. S., and Cooley, L. (2019) Proximity labeling reveals novel interactomes in live Drosophila tissue. *Development* **146**, dev176644

15. Packer, J. S., Zhu, Q., Huynh, C., Sivaramakrishnan, P., Preston, E., Dueck, H., Stefanik, D., Tan, K., Trapnell, C., Kim, J., Waterston, R. H., and Murray, J. I. (2019) A lineage-resolved molecular atlas of *C. elegans* embryogenesis at single-cell resolution. *Science* **365**, eaax1971

16. White, J. G., Southgate, E., Thomson, J. N., and Brenner, S. (1986) The structure of the nervous system of the nematode *Caenorhabditis elegans*. *Philos. Trans. R. Soc. Lond. B Biol. Sci.* **314**, 1–340

17. Taylor, S. R., Santpere, G., Reilly, M., Glenwinkel, L., Poff, A., McWhirter, R., Xu, C., Weinreb, A., Basavaraju, M., Cook, S. J., Barrett, A., Abrams, A., Vidal, B., Cros, C., Rafi, I., *et al.* (2019) Expression profiling of the mature *C. elegans* nervous system by single-cell RNA-sequencing. *bioRxiv.* https://doi.org/10.1101/737577

18. Lorenzo, R., Onizuka, M., Defrance, M., and Laurent, P. (2020) Combining single-cell RNA-sequencing with a molecular atlas unveils new markers for Caenorhabditis elegans neuron classes. *Nucleic Acids Res.* **48**, 7119–7134

19. Ge, M.-H., Wang, W., Wu, T.-H., Wen, X., Al-Sheikh, U., Chen, L.-L., Yin, S.-W., Wu, J.-J., Huang, J.-H., He, Q.-Q., Liu, H., Li, R., Wang, P.-Z., and Wu, Z.-X. (2020) Dual recombining-out system for spatiotemporal gene expression in *C. elegans*. *IScience* **23**, 101567

20. Bacaj, T., and Shaham, S. (2007) Temporal control of cell-specific transgene expression in *Caenorhabditis elegans*. *Genetics* **176**, 2651–2655

21. Nance, J., and Frøkjær-Jensen, C. (2019) The *caenorhabditis elegans* transgenic toolbox. *Genetics* **212**, 959–990

22. May, D. G., Scott, K. L., Campos, A. R., and Roux, K. J. (2020) Comparative application of BioID and TurboID for protein-proximity biotinylation. *Cells* **9**, 1070

23. Schäffer, U., Schlosser, A., Müller, K. M., Schäfer, A., Katava, N., Baumeister, R., and Schulze, E. (2010) SnAvi - a new tandem tag for high-affinity protein-complex purification. *Nucleic Acids Res.* **38**, e91

24. Waaijers, S., Muñoz, J., Berends, C., Ramalho, J. J., Goerdayal, S. S., Low, T. Y., Zoumaro-Djayoon, A. D., Hoffmann, M., Koorman, T., Tas, R. P., Harterink, M., Seelk, S., Kerver, J., Hoogenraad, C. C., Bossinger, O., *et al.* (2016) A tissue-specific protein purification approach in Caenorhabditis elegans identifies novel interaction partners of DLG-1/Discs large. *BMC Biol.* **14**, 1–24

25. Lobingier, B. T., Hu, R., Eichel, K., Miller, K. B., Ting, A. Y., Von Zastrow, M., Krogan, N. J., Lobingier, B. T., Hu, R., Eichel, K., Miller, K. B., Ting, A. Y., and Von Zastrow, M. (2017) An approach to spatiotemporally resolve protein interaction networks in living cells. *Cell* **169**, 350–360

26. Yuet, K. P., Doma, M. K., Ngo, J. T., Sweredoski, M. J., Graham, R. L. J., Moradian, A., Hess, S., Schuman, E. M., Sternberg, P. W., and Tirrell, D. A. (2015) Cell-specific proteomic analysis in Caenorhabditis elegans. *Proc. Natl. Acad. Sci. U. S. A.* **112**, 2705–2710

27. Aburaya, S., Yamauchi, Y., Hashimoto, T., Minakuchi, H., Aoki, W., and Ueda, M. (2020) Neuronal subclass-selective proteomic analysis in Caenorhabditis elegans. *Sci. Rep.* **10**, 1–9

28. Branon, T. C., Bosch, J. A., Sanchez, A. D., Udeshi, N. D., Svinkina, T., Carr, S. A., Feldman, J. L., Perrimon, N., and Ting, A. Y. (2018) Efficient proximity labeling in living cells and organisms with TurboID. *Nat. Biotechnol.* **36**, 880–898

29. Sanchez, A. D., Branon, T. C., Cote, L. E., Papagiannakis, A., Liang, X., Pickett, M. A., Shen, K., Jacobs-Wagner, C., Ting, A. Y., and Feldman, J. L. (2020) Proximity labeling at non-centrosomal organizing centers reveals VAB-10B and WDR-62 as distinct microtubule regulators. *bioRxiv.* https://doi.org/10.1101/2020.08.29.272369

30. Ortega-Cuellar, D., Hernandez-Mendoza, A., Moreno-Arriola, E., Carvajal-Aguilera, K., Perez-Vazquez, V., Gonzalez-Alvarez, R., and Velazquez-Arellano, A. (2010) Biotin starvation with adequate glucose provision causes paradoxical changes in fuel metabolism gene expression in rat (Rattus norvegicus), nematode (Caenorhabditis elegans) and yeast (Saccharomyces cerevisiae). *J. Nutrigenet. Nutrigenomics.* **3**, 18–30

31. Angeles-Albores, D., Raymond, R. Y., Chan, J., and Sternberg, P. W. (2016) Tissue enrichment analysis for *C. elegans* genomics. *BMC Bioinformatics* **17**, 1–10

32. Lockhead, D., Schwarz, E. M., O'hagan, R., Bellotti, S., Krieg, M., Barr, M. M., Dunn, A. R., Sternberg, P. W., and Goodman, M. B. (2016) The tubulin repertoire of Caenorhabditis elegans sensory neurons and its context-dependent role in process outgrowth. *Mol. Biol. Cell.* **27**, 3717–3728

33. Südhof, T. C. (2012) The presynaptic active zone. *Neuron* **75**, 11–25

34. Feinberg, E. H., VanHoven, M. K., Bendesky, A., Wang, G., Fetter, R. D., Shen, K., and Bargmann, C. I. (2008) GFP reconstitution across synaptic partners (GRASP) defines cell contacts and synapses in living nervous systems. *Neuron* **57**, 353–363

35. Carbonell, A. U., Cho, C. H., Tindi, J. O., Counts, P. A., Bates, J. C., Erdjument-Bromage, H., Cvejic, S., Iaboni, A., Kvint, I., Rosensaft, J., Banne, E., Anagnostou, E., Neubert, T. A., Scherer, S. W., Molholm, S., *et al.* (2019) Haploinsufficiency in the ANKS1B gene encoding AIDA-1 leads to a neurodevelopmental syndrome. *Nat. Commun.* **10**, 3529

36. Jordan, B. A., Fernholz, B. D., Khatri, L., and Ziff, E. B. (2007) Activity-dependent AIDA-1 nuclear signaling regulates nucleolar numbers and protein synthesis in neurons. *Nat. Neurosci.* **10**, 427–435

37. Jacob, A. L., Jordan, B. A., and Weinberg, R. J. (2010) Organization of amyloid-b protein precursor intracellular domain-associated protein-1 in the rat brain. *J. Comp. Neurol.* **518**, 3221–3236

38. Morrison, L. M., Edwards, S. L., Manning, L., Stec, N., Richmond, J. E., and Miller, K. G. (2018) Sentryn and SAD kinase link the guided transport and capture of dense core vesicles in caenorhabditis elegans. *Genetics* **210**, 925–946

39. Edwards, S. L., Morrison, L. M., Manning, L., Stec, N., Richmond, J. E., and Miller, K. G. (2018) Sentryn acts with a subset of active zone proteins to optimize the localization of synaptic vesicles in caenorhabditis elegans. *Genetics* **210**, 947–968

40. Loveless, T., Qadota, H., Benian, G. M., and Hardin, J. (2017) *Caenorhabditis elegans* SORB-1 localizes to integrin adhesion sites and is required for organization of sarcomeres and mitochondria in myocytes. *Mol. Biol. Cell.* **28**, 3621–3633
41. Brenner, S. (1974) The genetics of *Caenorhabditis elegans. Genetics* **77**, 71–94
42. Redemann, S., Schloissnig, S., Ernst, S., Pozniakowsky, A., Ayloo, S., Hyman, A. A., and Bringmann, H. (2011) Codon adaptation-based control of protein expression in *C. elegans. Nat. Methods* **8**, 250–252
43. Tyanova, S., Temu, T., and Cox, J. (2016) The MaxQuant computational platform for mass spectrometry-based shotgun proteomics. *Nat. Protoc.* **11**, 2301–2319

Murat Artan completed his PhD in South Korea at Postech and joined the de Bono lab first at the MRC Laboratory of Molecular Biology in Cambridge, UK, and then the Institute of Science and Technology (IST) Austria as a postdoc in life sciences. He studies molecular mechanisms of neuronal and neural circuit function using *C. elegans*. He became interested in applying proximity labeling to the worm nervous system and decided to share his optimized TurboID-based protocol with the *C. elegans* community as a resource paper.